The dielectric relaxation behaviour of m-fluoroaniline above the glass transition

M Cutroni, A Mandanici and A Piccolo

Dipartimento di Fisica Universita'di Messina and INFM, Contr. da Papardo, PO Box 55, 98166 Sant' Agata, Messina, Italy

Abstract. The dielectric properties of m-fluoroaniline have been investigated over seven decades of frequency (1 kHz–20 GHz) in the temperature range 188–303 K, above the calorimetric glass transition temperature. The Arrhenius plot of the inverse α peak frequencies reveals a non-linear character and a non-Debye relaxation function indicates a non-exponential temporal decay of the molecular polarization of the liquid near T_g. The dynamic behaviour turns out to be typical of highly fragile liquids and appears closely similar to that obtained from previous ultrasonic studies on the same system. A crossover between two distinct dynamical regimes takes place in the range of intermediate viscosity at a temperature T_c which falls about 40 K above the glass transition temperature T_g.

1. Introduction

The relaxation kinetics of fragile glass forming liquids [1,2] has been receiving much attention recently. In these systems, in fact, the phenomenology concerning the slowing down of particle motions and the related liquid–glass transition draws attention to special features whose explanation could shed light on the nature of this phenomenon [3].

Fragile glass formers are characterized by the strongest curvature in the Arrhenius plot of the shear viscosity and of the relaxation times involved in dielectric [4,5], mechanical [6,7], light scattering [8,9], or neutron spectroscopy [10,11]. In the high-viscosity regime ($\eta > 10^2$–10^3 poise) the deviation from the Arrhenius law is usually well described by the empirical Vogel–Fulcher–Tamman (VFT) equation

$$\eta(T) = A \exp\left[B/(T - T_0)\right] \qquad A, B > 0 \qquad 0 \leqslant T_0 < T_g \tag{1}$$

while in the low-viscosity regime ($\eta < 10^2$ poise) it turns out that power laws

$$\eta(T) = \eta_0 (T - T_0)^{-\gamma} \qquad \gamma \approx 2, 3 \qquad T_c \approx 1.3 T_g \tag{2}$$

are more suitable [12]. At the onset of supercooling, moreover, a breakdown of the Stokes–Einstein relation for diffusivity [13] and anomalies of the Debye–Waller factor [14,15] are generally found in spectroscopic experiments. For fragile systems, therefore, it is reasonable to suppose that a change in the mechanism of molecular mobility takes place in the range of intermediate viscosity. The understanding of the microscopic mechanism driving this crossover is of fundamental importance in that it constitutes the central prediction of theories based on entirely different approaches.

In the mode coupling theory (MCT) [16, 17] the dynamics evolve from a high-T regime ($T > T_c$) where collective motions are driven by coupled density fluctuations to a low-T regime ($T < T_c$) governed by thermally activated hopping processes. Although the inclusion of a 'jump' mechanism removes the ideal transition to non-ergodicity, claimed at T_c in the original formulation of the theory [18], T_c remains the most relevant temperature for liquid state dynamics and marks the boundary of different scaling regions for the α relaxation.

In the 'coupling model (CM)' of Ngai and coworkers [19, 20] the existence of two distinct dynamical regimes reflects the crossover of two time-scales: the time-scale $\bar{\tau}_0$, representing the relaxation time before existence of dynamical coupling among molecular relaxing units, and the 'renormalized' relaxation time τ^* when correlation becomes relevant. Dominance of one of the two regimes depends upon temperature through some correlation length $\xi(T)$, generally identified with the size of subregions in which molecular motions are cooperatively correlated (CRRs). In this approach thermodynamics factors drive the dynamic properties through the well known Adam–Gibbs equation [21]

$$\tau = A \exp(C/T S_c) \tag{3}$$

relating the configuration entropy of the supercooled liquid S_c to the rate of a structural rearrangement. This picture strikes against the MCT view of a dynamical origin of the glassy behaviour and advances an underlying thermodynamic phase transition at the Kauzmann temperature T_K [22].

Strong non-Debye relaxation is the other universal feature of fragile glass forming liquids [23]. The evolution to Debye relaxation, occurring generally at high temperatures, constitutes a fragility determining factor in the CM of Ngai but results in disagreement with the MCT prediction of a T-independent stretching above T_c. A strong temperature dependence of the non-exponentially parameter is also proposed in the percolation theory of Campbell *et al* [24]; here the liquid dynamics reflects the morphology of the accessible configuration space evolving from a high-T compact structure to a ramified percolating cluster near T_g.

To obtain physical insight into the scaling behaviour of the α relaxation process and into the fragile nature of m-fluoroaniline (m-FA) measurements of dielectric response over the radiowave and microwave frequency range have been performed from room temperature down to the glass transition point ($T_g = 173$ K, defined by differential scanning calorimetry (DSC) at 10 K min^{-1} [25]). In this way it is possible to verify the existence of two different regimes in the structural dynamics of this molecular liquid. Results are analysed in the framework of the above-discussed models and, further, compared with a previous ultrasonic investigation [26].

2. Experimental set-up and results

The measurement technique employed for the low frequencies has been discussed elsewhere [27]. The HP8720C vectorial network analyser with a dielectric probe for reflection measurements has been used above 50 MHz up to 20 GHz. The typical accuracy of this method is $\pm 5\%$ for the real permittivity and ± 0.005 for the loss tangent.

In figures 1 and 2 are shown the imaginary ε'', and real, ε' parts, respectively, of the complex dielectric permittivity over seven decades of frequency and at various fixed temperatures. The dielectric loss factor exhibits a well pronounced peak (α relaxation) that rapidly shifts through the experimental frequency window as temperature changes.
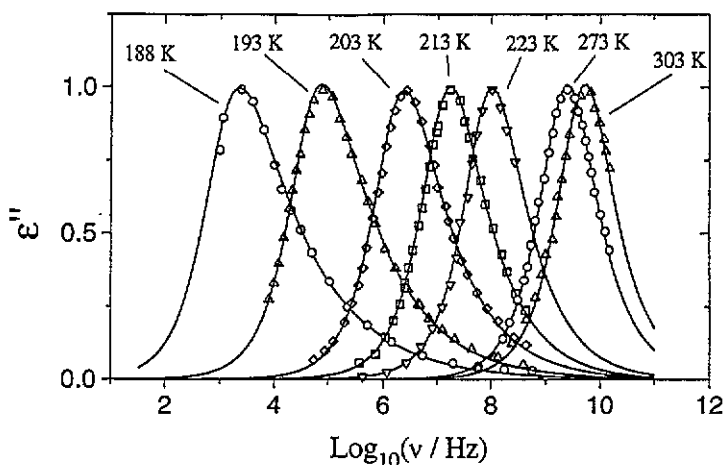
Figure 1. The imaginary part $\varepsilon''(\nu)$ of the dielectric permittivity of *m*-fluoroaniline as a function of frequency at selected temperatures. Peak heights have been normalized to unit. Solid lines have been obtained by fitting dielectric data to a Cole–Davidson equation.
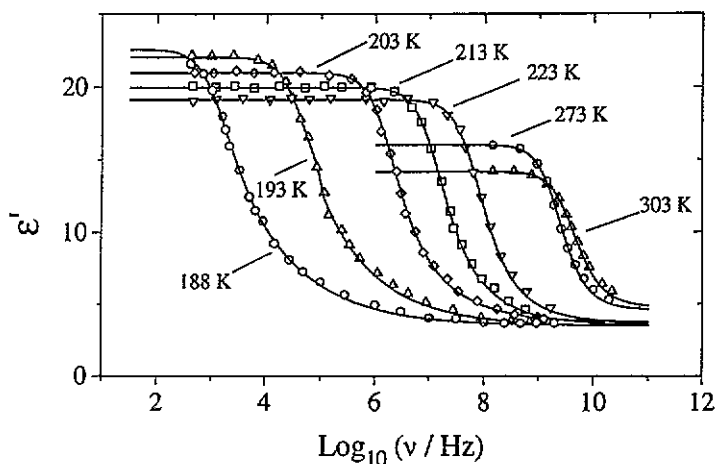
Figure 2. The real part $\varepsilon'(\nu)$ of the dielectric permittivity of *m*-fluoroaniline as a function of frequency at selected temperatures. Solid lines have been obtained by fitting dielectric data to a Cole–Davidson equation.

The permittivity shows correspondingly a strong dispersion decreasing from a static value, ε_0, typical of a liquid to a high-frequency value, ε_∞, characteristic of a solid. A least-squares fit of the data (the continuous lines in figures 1 and 2) has been obtained using the phenomenological Cole–Davidson expression

$$\varepsilon^*(\omega) = \varepsilon_\infty + \frac{\varepsilon_0 - \varepsilon_\infty}{(1 + i\omega\tau_{CD})^{\beta_{CD}}} \qquad 0 < \beta_{CD} \leqslant 1. \tag{4}$$

As it is evident in figure 1, this equation slightly fails in the high-frequency tails of the dielectric loss, a feature common to analogue systems such as glycerol and salol [28, 29]

and usually to all disordered systems. At low temperatures an asymmetric broadening of the relaxation with respect to a single Debye process produces the low values of the β_{CD} fit parameters. As temperature is raised, the deviation from Debye-like behaviour ($\beta_{CD} = 1$) becomes less significant and vanishes in the high-temperature/frequency region. Following the procedure described elsewhere [30] the β_{CD} parameters have been converted to β_{KWW} (the stretching parameter of the Kohlrausch function) and then a fit with the exponential growth function $\beta_{KWW} = 1 - \exp[-a(T - b)]$ ($a = 0.020\,19$ and $b = 151.7$) has been performed (figure 3). Extrapolation of the distribution parameter on this curve provides $\beta_{KWW}(T_g) = \frac{1}{3}$ (circled cross in figure 3) predicted by the Campbell percolation theory.
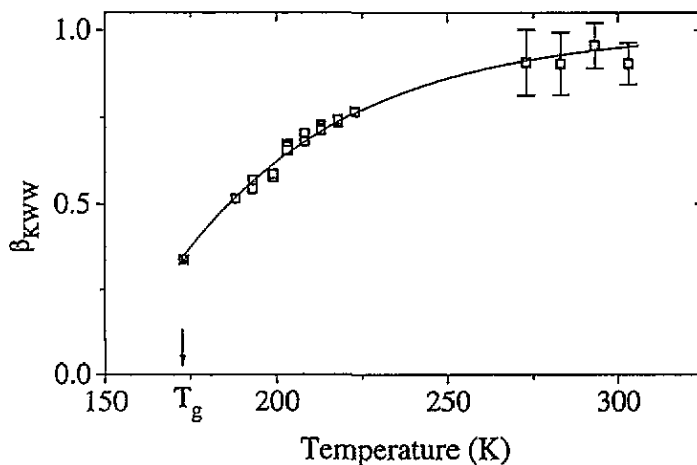

Figure 3. The Kohlrausch–Williams–Watt distribution parameter β_{KWW} as a function of temperature. The solid line has been obtained by fitting the β_{KWW} values to the exponential growth function $1 - \exp[-0.020\,19(T - 151.7)]$. The circled cross represents the limit glass transition value of the Campbell percolation theory: $\beta_{KWW} = \frac{1}{3}$.

In figure 4 the $\log_{10}$ of the inverse α peak frequencies plotted against the inverse temperature ($1000/T$) shows a pronounced non-linear character giving evidence of increasingly large deviations from the Arrhenius law as the temperature is decreased toward T_g. A single VFT form, $\tau = \tau_0 \exp[B/(T - T_0)]$, however, turns out to be unable to describe the whole range explored so it has been applied (fixing τ_0 to 5 ± 10^{-14} s) to fit only the low-temperature data. The curve clearly fails at high temperatures in the time-scale domain below 10^{-8}–10^{-9} s. In this temporal range the temperature dependence of τ_d seems to obey rather the power law proposed in the MCT $\tau = \tau_0(T - T_0)^{-\gamma}$ with $\gamma = 1.82$ and $T_c = 1.22$ (typical of very fragile glass forming liquids [31, 32]). For comparison, in figure 4 is also shown the best fit using the Arrhenius equation $\tau = \tau_0 \exp(E/k_B T)$ in the high-temperature range. The fit provides the value $E = 3.3$ kcal mol^{-1} for the activation energy. All the estimated values for the scaling parameters are listed in table 1.

3. Discussion

From the analysis of figure 4 it turns out that at least two fitting functions must be applied to describe the temperature dependence of the dielectric relaxation time τ_d. In the temperature
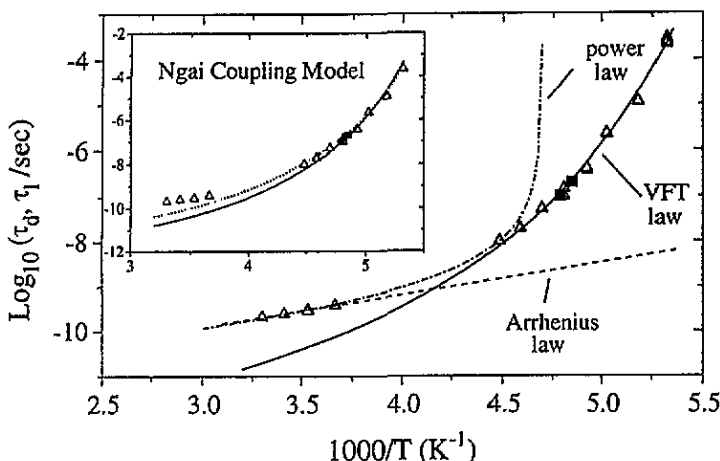
Figure 4. The $\log_{10}$ of the inverse ε'' peak frequencies ($\triangle$) as a function of the inverse temperature. Filled squares (■) are inverse mechanical α peak frequencies (5, 10 MHz) in the compliance formalism. The different fitting forms utilized are clearly indicated. The inset refers to the application of the coupling model of Ngai: full line, with the T_0 parameter free; dotted line, with T_0, A_0 and D_0 parameters free.

Table 1. Best fit parameters for the three different forms employed to describe the temperature dependence of the average dielectric and mechanical relaxation times.

VFT law (mechanical data) [26]		
τ_0 ($s \times 10^{15}$)	B (K)	T_0 (K)
6 ± 3	909 ± 10	140 ± 3
VFT law (dielectric data)		
τ_0 ($s \times 10^{14}$)	B (K)	T_0 (K)
5 ± 1	870 ± 15	149 ± 2
Power law (dielectric data)		
τ_0 ($s \times 10^{7}$)	T_c (K)	γ
6	212 ± 1	1.82
Arrhenius law (dielectric data)		
τ_0 ($s \times 10^{13}$)	E (kcal mol^{-1})	
8 ± 1	3.3	

range around $T_c = 212$ K the values of τ_d cross over from a power law to a VFT law T dependence, so it seems reasonable to affirm that T_c distinguishes two regimes of dielectric behaviour characterized by quite different relaxation mechanisms. The crossover temperature T_c is about 40 K higher than T_g and above it $\tau_d(T)$ can be well described by a power law with an exponent $\gamma = 1.82$, according to the MCT predictions. There is no evidence, however, of any analogue crossover in $\beta_{KWW}(T)$ at the same temperature and the rehological simplicity predicted for the α relaxation in the temperature range above T_c is not obeyed. After a rather fast initial increase, the β_{KWW} parameter effectively levels off but only at consistently higher temperatures than T_c, as is evident in figure 3. Regarding the low-T regime ($T < T_c$), it turns out that $\tau_d(T)$ does not display any return to Arrhenius behaviour, whose occurrence is a clear indication of the activity of phonon-assisted relaxation process.

As shown in the inset of figure 4, the CM of Ngai accounts well for the curvature (continuous line) at intermediate and low temperatures but shows deviations in the high-temperature region associated with the mesoscopic time domain ($\tau < 10^{-8}$–10^{-9} s). So, the high-viscosity/low-frequency regime of this liquid seems characterized by strongly correlated motions. Low β_{KWW} (large $n = 1 - \beta_{KWW}$) values, in fact, are associated with great intermolecular cooperativity, this parameter being interpreted as a measure of the coupling strength between a relaxing CRR and the complex system; non-Debye relaxation, therefore, should originate from effect of dynamic interactions according to the scheme

$$\Phi(t) = \begin{cases} \Phi(0)\exp[-(t/\bar{\tau}_0)] & \omega_c\bar{\tau}_0 \ll 1 \\ \Phi(0)\exp[-(t/\tau^*)^{1-n}] & \omega_c\bar{\tau}_0 \gg 1 \quad 0 < n < 1 \end{cases}. \tag{5}$$

The relaxation time $\bar{\tau}_0$ (associated with uncorrelated dynamics) is modified by the equation

$$\tau^*(T) = \left[(1-n)\omega_c^n\bar{\tau}_0\right]^{1/(1-n)} \tag{6}$$

to produce the experimentally observed T dependence and proves that the magnitude of n at T_g and its temperature variation $\mathrm{d}n/\mathrm{d}(T_g/T)$ are related to the extent of fragility of this system. In the fit procedure [20] the relation

$$\bar{\tau}_0 = A_0 \exp\left[D_0 T_0/(T - T_0)\right] \tag{7}$$

has been introduced into (6) using the values $A_0 = 2.147 \times 10^{-14}$ s and $D_0 = 12.7$ relative to glycerol (non-fragile liquid) and setting $\omega_c = 10^{11}$ s^{-1} (the value pertinent to molecular liquids). The coupling parameter $n(T) = 1 - \beta_{KWW}$ has been obtained utilizing the T dependence law determined in this work for the Kohlrausch exponent (see section 2). In this way, just T_0 has turned out to be a free parameter in the relation (6). Further release of the (material-dependent) Adam–Gibbs parameters D_0 and A_0 has not provided a much better fit of the high-temperature data, as is evident in the inset of figure 4 (dotted line). An explanation could be that the regions of cooperative rearrangement reach their typical size (~ 1, 2 nm) only at frequencies lower than 10^6–10^9 s^{-1} [33], for which, reasonably, the extent of intermolecular spatial correlation, embodied by n (or β_{KWW}), becomes important and constitutes a determining factor in generating fragile character. In the mesoscopic window ($\tau < 10^{-8}$–10^{-9} s), as a consequence, it seems that the time scaling behaviour of the α relaxation needs consideration of the hydrodynamic approach proposed in the MCT.

No evidence of decoupling between dielectric and mechanical (viscous) relaxation times has been found [1–3]. The inverse mechanical α peak frequencies (calculated in the compliance formalism $J'' = M''/(M'^2 + M''^2)$), in fact, overlap the dielectric ones (figure 4). So, the VFT parameters (see table 1) can be explained observing that in the first case they have been *directly* calculated fitting a set of inverse α peak frequencies while the available mechanical response at fixed frequency gave them *indirectly* [26]. On the other hand, the ultrasonic characterization of the β_{KWW} parameter turns out to be quite ambiguous and in [26] it had been arbitrarily assumed to be T independent. On this basis, the dielectric VFT values has been used to fit the ultrasonic data allowing, at the same time, the stretching parameter to be (linearly) temperature dependent. Following this procedure, a comparable χ^2 of the ultrasonic data best fit using only two free parameters rather than five has been obtained. Therefore, it is reasonable to suppose that the dielectric τ_d and the mechanical τ_l relaxation times have the same value and temperature dependence $\tau(T)$ over the range explored. Probably, in this liquid the same underlying mechanism 'relaxes'

different generalized stresses [34, 35]. As a consequence, the m-FA dynamical fragility $D = B/T_0 \approx 5.8$ is slightly higher than that deduced from ultrasonic measurements ($D \approx 6.5$). To compare the dielectric and mechanical relaxation widths the variable-temperature/fixed-frequency $\varepsilon_\nu''(T)$ ($\nu = 10$ MHz) curve has been constructed from the isothermal data of figure 1. The 10 MHz $\varepsilon_\nu''(T)$ and $J_\nu''(T)$ spectra have then been normalized to the common peak position ($T_{peak} = 208.9$ K) and maximum height (figure 5). The mechanical relaxation peak is broader than the dielectric one as in other liquids and disordered systems [36]. Probably, the dielectric probe couples via the dipole moment selectively while the mechanical interaction is more generalized.
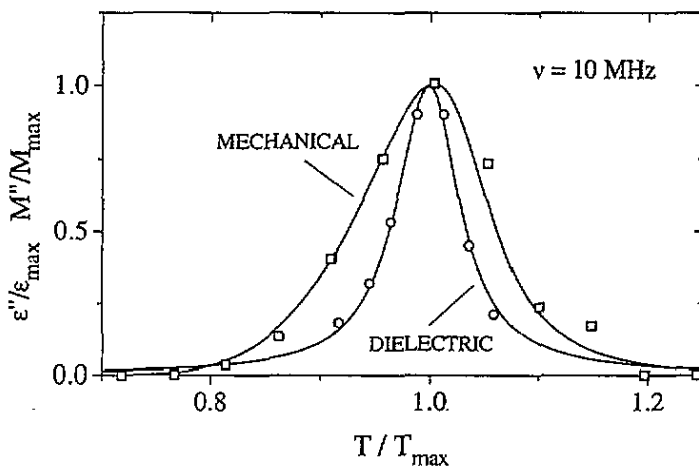

Figure 5. Comparison of the dielectric, ε'', and mechanical, M'', master curves as functions of temperature at the constant frequency of 10 MHz.

4. Conclusions

The investigation performed on molecular m-FA supports the existence of two regimes of dielectric behaviour separated by a crossover temperature T_c falling about 40 K above T_g. No single model has been able to account for this transition of dynamic domains. From the analysis of the experimental data it emerges that the hydrodynamic approach proposed by the MCT may be plausible at high temperatures but, when the high-viscosity regime is approached, the α relaxation cannot be explained without considering the liquid as a complex correlated system. In this temperature range, in particular, it is found that the curvature of τ_d depends critically on the magnitude and temperature variation of β_{KWW}, which, at the same time, successfully verifies the quantitative prediction of the Campbell percolation theory. Both these models state that the α relaxation time scaling behaviour turns out to be an implication of the evolving topology of the accessible points in the configuration space. So, the temperature dependence of β_{KWW} and the kinetic singularity implied by the VFT law (universal of the dielectric response) seem to bring to light the existence of a diverging length scale at decreasing temperatures. From the present analysis therefore, it seems that the problem of dielectric relaxation of fragile liquids in their strongly supercooled regime requires the approach of cooperativity and probably must be resolved on a thermodynamic basis.

References

[1] Angell C A 1988 *J. Non-Cryst. Solids* **102** 205
[2] Angell C A 1991 *J. Non-Cryst. Solids* **131–133** 13
[3] Angell C A 1988 *J. Phys. Chem. Solids* **49** 863
[4] Schönhals A, Kremer F and Schlosser E 1991 *Phys. Rev. Lett.* **67** 999
[5] Wu L 1991 *Phys. Rev.* B **43** 9906
[6] Jeong Y H, Nagel S R and Bhattacharya S 1986 *Phys. Rev.* A **34** 602
[7] Jeong Y H 1987 *Phys. Rev.* A **36** 766
[8] Du W M, Li G, Cummins H Z, Fuchs M, Toulouse J, Knauss L and Tao A 1994 *Phys. Rev.* E **49** 2192
[9] Li G, Du W M, Sakai A and Cummins H Z 1992 *Phys. Rev.* A **46** 3343
[10] Börjesson L, Elmroth M and Torell L M 1991 *J. Non-Cryst. Solids* **131–133** 139
[11] Börjesson L and Howells W S 1991 *J. Non-Cryst. Solids* **131–133** 53
[12] Taborek P, Kleiman R N and Bishop D J 1986 *Phys. Rev.* B **34** 1835
[13] Rössler E 1990 *Phys. Rev. Lett.* **65** 1595
[14] Börjesson L, Elmroth M and Torell L M 1990 *Chem. Phys.* **149** 209
[15] Börjesson L, Elmroth M and Torell L M 1992 *Phys. Rev. Lett.* **68** 79
[16] Götze W and Sjögren L 1988 *J. Phys. C: Solid State Phys.* **21** 3407
[17] Bengtzelius U, Götze W and Sjolander A 1984 *J. Phys. Chem.* **17** 5915
[18] Leutheusser E 1984 *Phys. Rev.* A **29** 2765
[19] Rajagopal A K, Ngai K L and Teitler S 1991 *J. Non-Cryst. Solids* **131–133** 282
[20] Ngai K L, Rendell R W and Plazek D J 1991 *J. Chem. Phys.* **94** 3018
[21] Adam G and Gibbs J H 1965 *J. Chem. Phys.* **43** 139
[22] Kauzmann W 1948 *Chem. Rev.* **43** 219
[23] Hunt A 1993 *J. Non-Cryst. Solids* **160** 183
[24] Campbell I A, Flesselles J-M, Jullien R and Botet R 1988 *Phys. Rev.* B **37** 3825
[25] Alba-Simionescu C, Busse L E, List D J and Angell C A 1990 *J. Chem. Phys.* **92** 617
[26] Cutroni M, Migliardo P, Piccolo A and Alba-Simionescu C 1994 *J. Phys.: Condens. Matter* **6** 5283
[27] Cutroni M, Mandanici A, Piccolo A and Alba-Simionescu C 1994 *Nuovo Cimento* D **16** 933
[28] Menon N, O'Brien K P, Dixon P K, Wu L, Nagel S R, Williams B D and Carini J P 1990 *J. Non-Cryst. Solids* **141** 61
[29] Dixon P K, Wu L, Nagel S R, Williams B D and Carini J P 1990 *Phys. Rev. Lett.* **65** 1108
[30] Lindsey C P and Patterson G D 1980 *J. Chem. Phys.* **73** 3348
[31] Schönhals A, Kremer F, Hoffmann A, Fischer E W and Schlosser E 1993 *Phys. Rev. Lett.* **70** 3459
[32] Rössler E 1991 *J. Non-Cryst. Solids* **131–133** 242
[33] Donth E 1982 *J. Non-Cryst. Solids* **53** 325
[34] Wu L, Dixon P K, Williams B D and Carini J P 1991 *J. Non-Cryst. Solids* **131–133** 32
[35] Dixon P K 1990 *Phys. Rev.* B **42** 8179
[36] Ngai K L 1994 *Evidences for Universal Behaviour of Condensed Matter at Low Frequencies/Long Times* (Washington, DC: Naval Research Laboratory) and cited in Richert R and Blumen A (ed) 1994 *Universal Patterns of Relaxation in Complex Correlated Systems* (Berlin: Springer) p 23